Design and Construction of Curved Support Structures with Repetitive Parameters

Eike Schling[1], Martin Kilian[2], Hui Wang[2,3], Jonas Schikore[1], Helmut Pottmann[2]

[1] Chair of Structural Design
Technical University of Munich, Munich, Germany
(eike.schling | jonas.schikore)@tum.de

[2] Institute of Discrete Mathematics and Geometry
Vienna University of Technology, Vienna, Austria
(kilian | hwang | pottmann)@geometrie.tuwien.ac.at

[3] School of Mathematical Sciences
Dalian University of Technology, Dalian City, P.R.C.

Abstract

The fabrication and construction of curved beams along freeform skins pose many challenges related to their individual and complex geometry. One strategy to simplify the fabrication process uses elastic deformation to construct curved beams from flat elements. Controlling the curvature of the design surface and beams has the additional potential to create repetitive building parts with beneficial beam orientation.

We aim for strained gridshells built entirely from straight or circular lamellas of the same radius and with orthogonal nodes. The lamellas are aligned normal to a reference surface enabling an elastic assembly via their weak axis and a local transfer of loads via their strong axis.

We show that the corresponding reference surfaces are of constant mean curvature and that the network of beams bisects principal curvature directions. We introduce a new discretization of these networks as quadrilateral meshes with spherical vertex stars and present a computational workflow for the design of such structures.

The geometric advantages of these networks were key for the fabrication and assembly of a prototype structure, the Asymptotic Gridshell. We describe the complete process from design to construction, presenting further insights on the symbiosis of geometry, fabrication and load-bearing behavior.

Key words: curved support structures, CMC-surfaces, elastic deformation, developable surfaces, strained gridshell, asymptotic curves, minimal surfaces, FEM
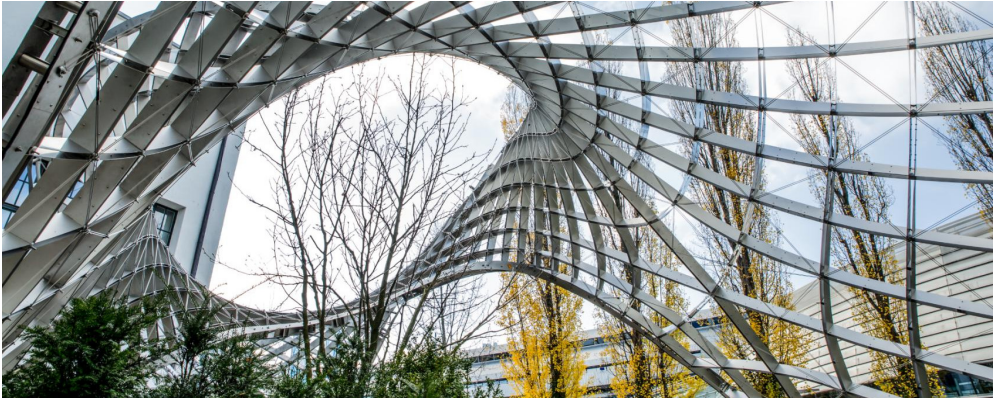
Figure 1: The Asymptotic Gridshell was designed for a green courtyard encompassing a central tree. The strained gridshell was assembled with orthogonal nodes from straight and flat lamellas, and erected elastically. *(Image: Felix Noe)*

1 Introduction

Gridshells are highly efficient structures because they carry loads through their curved shape with very little material. Their construction however, poses great challenges related to their complex geometry. In a freeform grid every node and every beam are likely to be different and have to be fabricated individually using computer aided, 3D manufacturing tools. Controlling the curvature parameters of design surfaces and beam networks, and using the elastic behavior of material to shape these grids opens up new strategies for fabrication-aware design.

We study structures that can be constructed with *congruent nodes* from lamella that are *orientated normal* to the underlying reference surface and have *straight* or *circular development* (Figure 1). The slender lamellas allow for an elastic assembly via their weak axis and a local transfer of loads via their strong axis. The lamella network can be transformed elastically following a predetermined kinetic behavior. This enables a simple erection process without formwork. The final grid forms a doubly-curved network, enabling an efficient, spatial load transfer as a shell structure. We are interested in the possible shapes, their computational design and solutions for construction.

Related work.   We follow up on recent work by Tang et al. (2016) on curved support structures from developable strips. A prominent example of this type is provided by the Eiffel Tower Pavilions (Schiftner et al. (2012), Figure 2). However, this support structure follows principal curvature lines and does not lead to lamellas with straight or circular development. The design of strained grid structures with the use of developable strips has been investigated by Schling and Barthel (2017).

From the construction perspective our approach is inspired by the strained timber gridshells of Frei Otto (Burkhardt (1978)), namely, the Multihalle in Mannheim, see Figure 2.
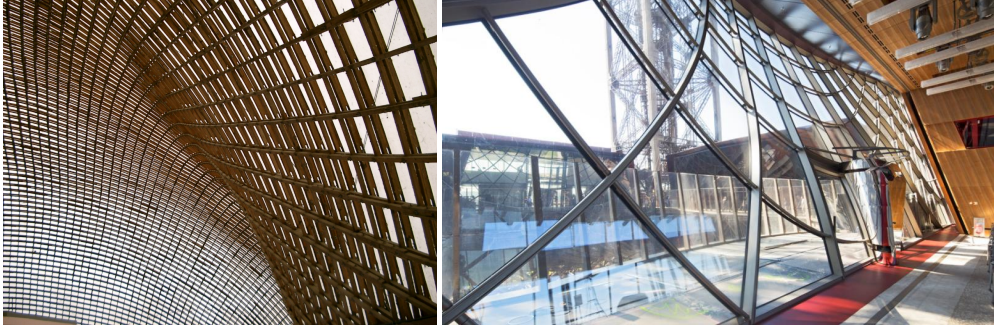
Figure 2: Curved grid structures: Left: Multihalle Mannheim by Frei Otto, 1975. The strained timber gridshell is formed from elastically-bent timber laths. Right: The Eiffel Tower Pavilions by Moatti Rivière Architects. The facade structure follows the principal curvature directions. The curved steel beams were fabricated from flat strips of steel.
(Images: Rainer Barthel, Michel Denancé)

Overview and contribution. We show that the requirements on lamellas and nodes lead to special curve networks on surfaces. Circular lamellas of constant radius and right node angles live on surfaces of constant-mean-curvature (CMC). Our computations use a novel discrete representation, namely quadrilateral meshes with *spherical vertex stars*. They generalize the well-known asymptotic nets with planar vertex stars (Bobenko and Suris (2008)).

We present a method for the computation of isothermic networks on CMC surfaces. The diagonals of such a network form curves of constant normal curvature κ_n and define the attachment points of lamellas of radius $r = 1/\kappa_n$ with 90 degree intersection angles. This includes the special case of straight lamellas with $r = \infty$.

The implications of planning and constructing such networks for a load-bearing gridshell are described in Section 3. Our case study, the Asymptotic Gridshell, was designed using asymptotic curves (vanishing normal curvature) on a minimal surface (zero mean curvature) and constructed from straight lamellas and orthogonal nodes. We discuss the architectural design process of surface and network, introduce a detail solution for a typical grid-joint, and present the fabrication and erection process. The load-bearing behavior is analyzed using a novel workflow to simulate residual stresses.

2 Theory and computation

Let us briefly recall a few facts from differential geometry. It will be helpful to know about the *Darboux frame* which is attached to a curve $\mathbf{c}$ on a surface S. Let $\mathbf{c}(s)$ be an arc length parametrization of that curve. At each point $\mathbf{c}(s)$, the Darboux frame consists of the unit tangent vector $\mathbf{t}(s)$, the unit vector $\mathbf{n}(s)$ orthogonal to the surface S, and the sideways vector $\mathbf{u}(s) = \mathbf{n}(s) \times \mathbf{t}(s)$, see Figure 3. As the frame
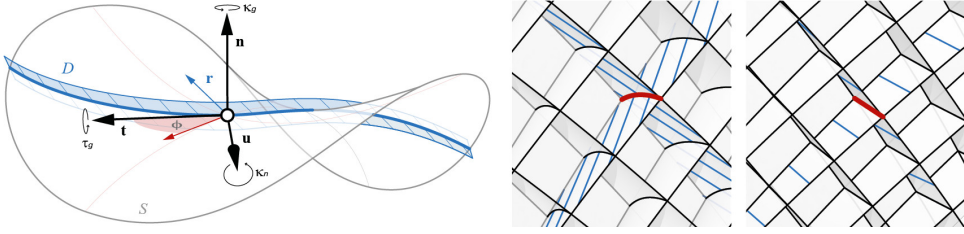
Figure 3: A developable strip attached orthogonally to a surface S along $\mathbf{c}$. Its rulings $\mathbf{r}$ are generally not parallel to the normal vector $\mathbf{n}$. This results in curved intersections of strips.

moves along the curve, at any time s the angular velocity vector $\mathbf{d}$ is given by

$$\mathbf{d} = \tau_g \mathbf{t} - \kappa_n \mathbf{u} + \kappa_g \mathbf{n}.$$

Its coefficients are important quantities of the surface curve $\mathbf{c}$: *geodesic curvature* κ_g, *normal curvature* κ_n and *geodesic torsion* τ_g. The derivatives of the frame vectors with respect to s satisfy $\mathbf{t}' = \mathbf{d} \times \mathbf{t}$, $\mathbf{u}' = \mathbf{d} \times \mathbf{u}$, $\mathbf{n}' = \mathbf{d} \times \mathbf{n}$. Inserting the above expression for $\mathbf{d}$, one finds

$$\kappa_g = \mathbf{t}' \cdot \mathbf{u}, \ \ \kappa_n = \mathbf{t}' \cdot \mathbf{n}, \ \ \tau_g = \mathbf{u}' \cdot \mathbf{n}.$$

Thus, κ_g and κ_n are the tangential and normal components of the curvature vector $\mathbf{t}'$, and τ_g is the normal component of $\mathbf{u}'$.

The geometric model of a curved support structure is a network of developable surface strips which are orthogonal to a reference surface S. Let us consider such a developable strip D, attached to S along the common curve $\mathbf{c}$. If we want to make a model from originally straight flat strips, the curve $\mathbf{c}$ must map to a straight line in the planar unfolding of D. This means that $\mathbf{c}$ has to have vanishing geodesic curvature with respect to D. At each point of $\mathbf{c}$, the tangent planes of D and S are orthogonal. Therefore, $\mathbf{c}$ has vanishing normal curvature with respect to S; it is a so-called *asymptotic curve* on S.

We will also study models from strips whose flat developments are circular. In order to achieve a circle of radius r as the image of $\mathbf{c}$ in the flat development of D, $\mathbf{c}$ must have constant geodesic curvature $1/r$ with respect to D and therefore *constant normal curvature* $1/r$ with respect to the reference surface S.

Let us summarize these important facts: *A flat circular strip which is subject to bending and no stretching can be attached orthogonally to a given surface S only along a curve $\mathbf{c}$ of constant normal curvature. In particular, a straight strip can only be attached orthogonally along an asymptotic curve of S.*

The developable surface D which is orthogonal to S along $\mathbf{c}$ is in general not formed by the surface normals along $\mathbf{c}$. The surface D is enveloped by planes orthogonal to S and tangent to $\mathbf{c}$, but its straight lines (rulings) are in general not orthogonal to S (Figure 3). As discussed in detail by Tang et al. (2016), the ruling vectors are given

by $\mathbf{r} = \kappa_g \mathbf{n} + \tau_g \mathbf{t}$ and thus agree with the surface normal $\mathbf{n}$ for $\tau_g = 0$, which in most of our examples is not the case. Related to this fact is the following one: The strips intersect at a node along a curve $\bar{\mathbf{n}}$ and not in the surface normal (Figure 3, right). However, this curve $\bar{\mathbf{n}}$ is usually nearly straight and for practical purposes may be approximated by a straight line. We will also talk about a *node angle*, which refers to the one measured directly at the reference surface S. Theoretically, the angle between the two strips differs slightly along $\bar{\mathbf{n}}$.

To have more repetition in parameters, one may want to achieve the same node angle for all nodes. To discuss this, we need Euler's formula for the distribution of normal curvatures at a surface point:

$$\kappa_n = \kappa_1 \cos^2 \phi + \kappa_2 \sin^2 \phi.$$

Here, κ_1, κ_2 are the two principal curvatures and ϕ is the angle between the first principal curvature and the direction for which we compute the normal curvature κ_n. Directions with the same normal curvature are symmetric with respect to the principal directions as they are represented by ϕ and $-\phi$. If we want a constant right node angle and work with strips of the same radius in the development, the two directions meeting at a node are given by $\phi = \pm\pi/4$ and therefore $\kappa_n = (\kappa_1 + \kappa_2)/2 = H$, H denoting *mean curvature*. This means that such a structure can only realize surfaces S for which the mean curvature equals $1/r$. These CMC surfaces are very well studied in differential geometry. A special case occurs when we use straight strips $(r = \infty)$, where we obtain $H = 0$ and thus *minimal surfaces*.

CMC surfaces are a mathematical representation of inflated membranes, such as soap bubbles or pneus. Their curvature behavior corresponds to the equilibrium shape caused by a pressure difference and can form both synclastic and anticlastic surface regions. Minimal surfaces are a subset of CMC surfaces, in which the pressure difference is zero. They can be found in nature in the form of soap films, creating the minimal area within given boundaries.

We have just derived another important fact: *Curved support structures from circular strips of the same radius r and with a right node angle model surfaces with constant mean curvature $H = 1/r$; in particular, straight strips yield models of minimal surfaces. The strips of the support structure are attached along those curves which bisect the principal directions.* These bisecting directions are those with extremal geodesic torsion.

CMC surfaces, and in particular minimal surfaces, are so-called *isothermic surfaces*. They possess a parameterization $\mathbf{s}(u, v)$ in which the isoparameter lines are principal curvature lines and which describes a conformal (angle preserving) mapping from the (u, v)-parameter plane to the surface. This parameterization maps the bisecting grid $u \pm v = $ const. onto those curves along which our strips can be attached. This fact is used later in our algorithm.

If we require a constant, but not necessarily right node angle 2ϕ, Euler's formula shows that the surface S possesses a linear relation between its principal curvatures,
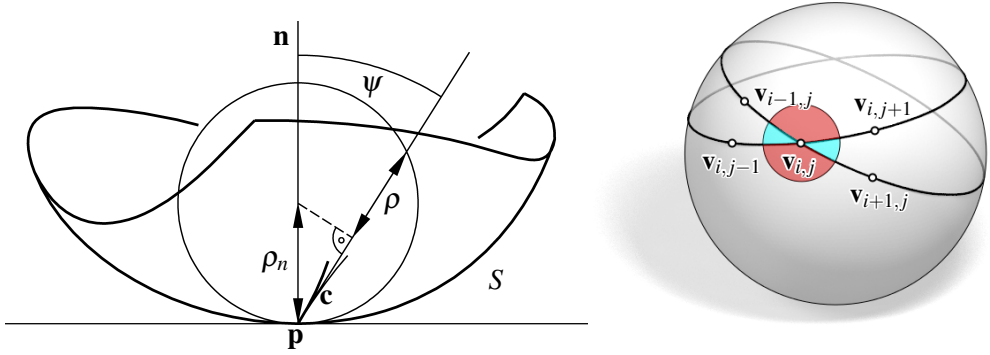
Figure 4: Left: Meusnier's theorem, relating the curvature of a curve $\mathbf{c}$ passing through $\mathbf{p}$ to normal curvature at $\mathbf{p}$ in direction of $\mathbf{c}'$. Right: Spherical vertex star.

$A\kappa_1 + B\kappa_2 = 1/r$, with $A = \cos^2\phi$, $B = \sin^2\phi$. Structures from straight strips $(r = \infty)$ lead to surfaces with a constant negative ratio of principal curvatures $\kappa_1/\kappa_2 = -B/A$. Those have recently been studied by Jimenez et al. (2018).

2.1 Discretization

For digital design of the structures we have in mind, it is very useful to have discrete models of the network of curves along which the strips are attached. This means that we have to come up with quad meshes whose mesh polylines discretize the system of curves of constant normal curvature κ_n on a smooth surface.

It is useful to know about Meusnier's formula and its geometric interpretation (see Figure 4). The formula relates curvature κ of a curve $\mathbf{c}$ on a surface to its normal curvature κ_n via $\kappa_n = \kappa \cos\psi$, where ψ is the angle between the curve's osculating plane and the surface normal. Geometrically, this means that the osculating circle of $\mathbf{c}$ (which has radius $\rho = 1/\kappa$) lies on a sphere of radius $\rho_n = 1/\kappa_n$, which is tangent to the surface. Note that κ_n only depends on the tangent direction. Hence, all curves on a surface which pass through a given point $\mathbf{p}$ with a fixed tangent possess osculating circles at $\mathbf{p}$ which lie on the corresponding Meusnier sphere. This knowledge allows us to prove the following fact:

A quad mesh of regular combinatorics for which each vertex and its four connected neighbors lie on a sphere of constant radius r, discretizes a network of curves of constant normal curvature $1/r$ on a smooth surface.

For a proof, we consider a vertex $\mathbf{v}_{i,j}$ and its four connected neighbors $\mathbf{v}_{i-1,j}$, $\mathbf{v}_{i+1,j}$, $\mathbf{v}_{i,j-1}$, and $\mathbf{v}_{i,j+1}$ (see Figure 4). By our assumption, these 5 points lie on a sphere $S_{i,j}$ of radius r. The three points $\mathbf{v}_{i-1,j}$, $\mathbf{v}_{i,j}$, $\mathbf{v}_{i+1,j}$ are consecutive points on a discrete parameter line and lie on a circle, which is a discrete version of the osculating circle of that parameter line at $\mathbf{v}_{i,j}$. Of course, this circle lies on $S_{i,j}$. Likewise, the three points $\mathbf{v}_{i,j-1}$, $\mathbf{v}_{i,j}$, $\mathbf{v}_{i,j+1}$ define a discrete osculating circle for the other discrete parameter line, which also lies on $S_{i,j}$. These osculating circles can be seen as tangent to an underlying surface and thus we see that the sphere $S_{i,j}$ is

tangent to that surface and contains the osculating circles. Hence, it is the common Meusnier sphere to the two parameter lines through $\mathbf{v}_{i,j}$. As all these vertex spheres have radius r, we have a discretization of the network of curves of constant normal curvature $1/r$.

In order to achieve a right angle in the discrete sense we require that the sum of opposite angles around $\mathbf{v}_{i,j}$ is equal (Figure 4, right). This discrete orthogonality condition is also used for conical meshes (Liu et al. (2006)). If we apply the right angle condition in addition to the sphere condition, we obtain a new discretization of CMC surfaces. Only in the special case of $r = \infty$, where the spheres degenerate to planes, do we arrive at a known asymptotic discretization of minimal surfaces.

A careful study of meshes with vertex spheres (not necessarily of constant radius) and their special cases is left for future research; it is more a topic of discrete differential geometry rather than architectural geometry.

2.2   Implementation

A key step is the computation of isothermic networks on CMC surfaces. Networks are represented as quad dominant meshes. An isothermic mesh M on top of a reference surface S is characterized by (i) edges aligned to principal curvature directions of S and (ii) quadrilateral faces that are as square as possible. As mentioned above, such networks always exist on CMC surfaces. The main difference between two such networks on the same CMC surface is the size of the squares.

Approach.   We start from an initial quad mesh whose edges are aligned to principal curvature directions of a reference CMC surface S. If such a mesh M_0 cannot be created with the help of a known parametrization of S, we use T.MAP (Evolute GmbH (2018)) to initialize M_0.

We iteratively deform M_0 to an isothermic mesh by letting it slide along principal curvature directions of S until all faces are as square as possible; we refer to this process as *straightening*. Note that straightening does not provide a solution to the difficult problem of singularity resolution since it does not change mesh combinatorics.

The main tool used during straightening is so-called *guided projection* as introduced by Tang et al. (2014). Guided projection allows us to prescribe a set of constraints in terms of vertex coordinates, face normals, curvature directions, and other mesh/surface-related quantities. A solution to this set of constraints yields an isothermal mesh M_1 to which we apply mid-edge subdivision in order to obtain a mesh M_2 whose edges are aligned to directions of constant normal curvature on S (see Figure 5 for an illustration). If the density of curves is not chosen with care, the resulting isothermic mesh may only cover part of S as illustrated in the small inset. In this example we added additional horizontal curves and let the straightening process distribute them across the surface. As a rule of thumb, it is beneficial to
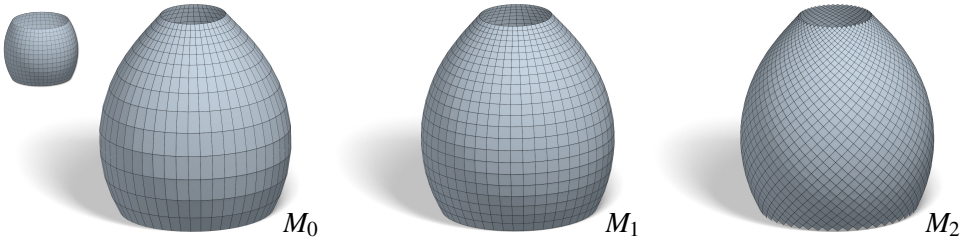
Figure 5: *From left to right: Principal but not yet isothermic mesh on an unduloid surface. Straightening deforms the rectangles of M_0 into squares of M_1. Mid-edge subdivision yields a mesh M_2 with edge polylines aligned to directions of constant normal curvature on the unduloid.*

have a reference surface S larger than the actual structure to give the straightening process enough room.

We lay out strips orthogonal to S along each polyline of constant normal curvature of M_2. To this end we use the corresponding normals of the reference surface S as initial rulings. Those strips are not yet developable and are subject to optimization via guided projection.

Guided projection. In a nutshell, guided projection takes a set of simultaneous equations and 'solves' them by performing Gauss-Newton iterations. The important observation made by Tang et al. (2014) is that this simple idea performs especially well if the involved equations are, at most, quadratic in the unknowns. We will not go into detail of the Gauss-Newton algorithm and refer to Tang et al. (2014). In the remainder of this section we will talk about the actual equations that we use.

Given a polygonal mesh M, its vertex coordinates $\mathbf{v}_i$, $i = 1, \ldots, n$, define our main set of variables. All other quantities, such as face normals etc., are derived quantities that are tied to vertex coordinates via equations. To transform M into a mesh with planar faces f_j, $j = 1, \ldots, m$, we introduce the vertex normals $\mathbf{n}_j$ as additional variables and the equations

$$1 = \mathbf{n}_j^T \mathbf{n}_j$$
$$0 = \mathbf{n}_j^T (\mathbf{v}_{i_2} - \mathbf{v}_{i_1})$$

where j run over all faces f_j of M and the pair $(\mathbf{v}_{i_1}, \mathbf{v}_{i_2})$ runs over all edges of f_j. A mesh that satisfies these equations has planar faces f_j and corresponding normal vectors $\mathbf{n}_j$. We use these *planarity constraints* to make a quad strip developable.

Recall that we are not trying to solve a form finding problem: the vertices $\mathbf{v}_i$ are constrained to move on S. We can implement this restriction by introducing equations of the form

$$0 = \left(\mathbf{m}_i^T (\mathbf{v}_i - \mathbf{p}_i) \right)^2 + \varepsilon \|\mathbf{v}_i - \mathbf{p}_i\|^2$$

where $\mathbf{p}_i$ is the footpoint of $\mathbf{v}_i$ on S and $\mathbf{m}_i$ is the normal of S at $\mathbf{p}_i$. This is commonly referred to as *tangent-distance-minimization* and restricts the movement of $\mathbf{v}_i$ to
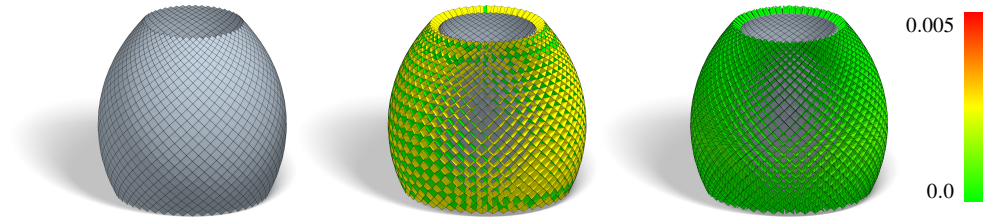
Figure 6: From left to right: Base mesh aligned to curves of constant normal curvature. Initial set of strips, color coded according to developability. Post optimized strips after one round of subdivision and 20 iterations of guided projection.

the tangent plane of S at $\mathbf{p}_i$. Note that $\mathbf{p}_i$ and $\mathbf{m}_i$ are not treated as variables – their values are updated between Gauss-Newton iterations.

With the help of the projection operator we can also achieve alignment of mesh edges to prescribed directions – in our case directions of principal curvature which are precomputed on S. We project the midpoint of edge $(\mathbf{v}_i, \mathbf{v}_j)$ onto S to obtain the principal curvature directions $\mathbf{d}_1$ and $\mathbf{d}_2$. The edge $(\mathbf{v}_i, \mathbf{v}_j)$ should be aligned to one of those directions. The corresponding *alignment equation* reads

$$0 = \mathbf{d}_1^T(\mathbf{v}_i - \mathbf{v}_j)\mathbf{d}_2^T(\mathbf{v}_i - \mathbf{v}_j) = (\mathbf{v}_i - \mathbf{v}_j)^T\mathbf{d}_1\mathbf{d}_2^T(\mathbf{v}_i - \mathbf{v}_j).$$

To obtain a *conformal parametrization* we use an equation introduced in the context of circle packings (Schiftner et al. (2009)). For each vertex $\mathbf{v}_i$ we introduce a scalar variable $l_i > 0$ and the equations

$$0 = (\mathbf{v}_i - \mathbf{v}_j)^T(\mathbf{v}_i - \mathbf{v}_j) - (l_i + l_j)^2$$

where j runs over all neighbors of vertex $\mathbf{v}_i$.

Optimizing discrete structures typically requires a *fairing term* to ensure overall mesh quality. When dealing with quadrilateral meshes it is sufficient to require that a generic vertex $\mathbf{v}_{i,j}$ (cf. Figure 4) and its four neighbors satisfy

$$2\mathbf{v}_{i,j} = \mathbf{v}_{i-1,j} + \mathbf{v}_{i+1,j}$$
$$2\mathbf{v}_{i,j} = \mathbf{v}_{i,j-1} + \mathbf{v}_{i,j+1}.$$

Finally, we may want to optimize a given mesh towards a mesh with *spherical vertex stars* as explained above. For each vertex we introduce a radius r_i, sphere center $\mathbf{c}_i$, and equation

$$0 = (\mathbf{v}_i - \mathbf{c}_i)^T(\mathbf{v}_i - \mathbf{c}_i) - r_i^2.$$

A neighboring vertex $\mathbf{v}_j$ has to satisfy $0 = (\mathbf{v}_j - \mathbf{c}_i)^T(\mathbf{v}_j - \mathbf{c}_i) - r_i^2$.

2.3 Results

We start with a remark on the color coding of strips in this section. To judge the developability of a quad strip we measure the planarity of individual quads
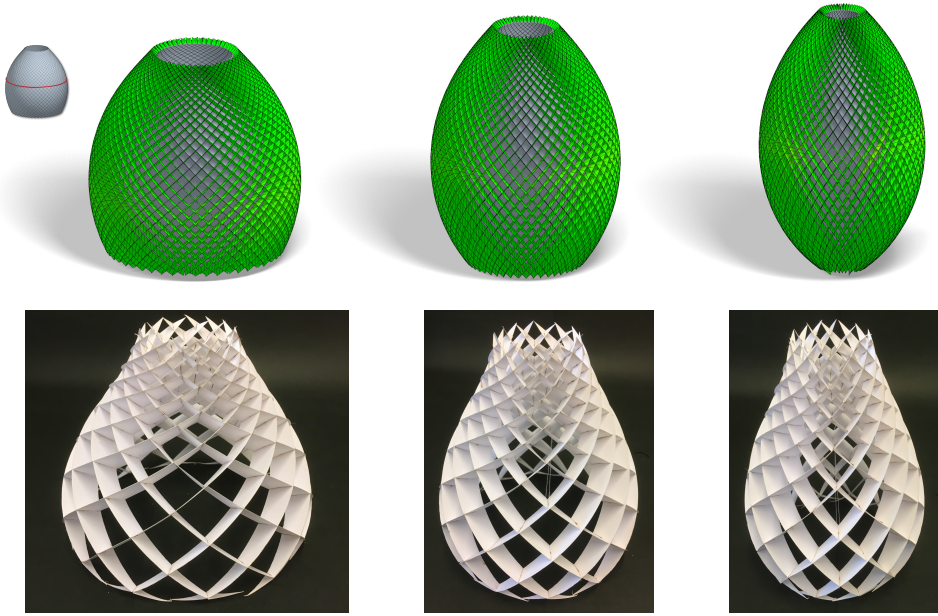
Figure 7: Deformation of the unduloid using the spherical vertex star property. The radius of the red curve was reduced by 10, respectively 20% to drive the deformation. The bottom row shows a corresponding paper model employing a coarser curve network on the upper half of the unduloid.

$(\mathbf{v}_1, \mathbf{v}_2, \mathbf{v}_3, \mathbf{v}_4)$ as the distance of its diagonals. To factor out scaling this number needs to be normalized. To do this we divide by the mean length of diagonals and arrive at the following planarity score:

$$\mathsf{ps}(\mathbf{v}_1, \mathbf{v}_2, \mathbf{v}_3, \mathbf{v}_4) = \frac{2d(\overline{\mathbf{v}_1\mathbf{v}_3}, \overline{\mathbf{v}_2\mathbf{v}_4})}{d(\mathbf{v}_1, \mathbf{v}_3) + d(\mathbf{v}_2, \mathbf{v}_4)}.$$

If we imagine a 1×1 m square, a diagonal distance of 1 cm maps to a planarity score of about 0.007. When applying color, pure red maps to a planarity score of 0.005 or higher.

Starting from an initial quad mesh M aligned to principal curvature directions of a reference surface S, we used the fairness, alignment, and conformality constraints while restricting movement to S via the closeness term to turn M into an isothermic mesh. The diagonals of M define the contact curves along which strips are attached. Strips are optimized for developability using the planarity constraint while constraining their lower boundary curves to S and their upper boundaries to a parallel surface at prescribed distance h.

Unduloid. The unduloid is obtained as a surface of revolution of an elliptic catenary. Figure 6 shows a network of curves with constant normal curvature, an initial set of strips using surface normals of a triangle mesh representation as node axis, and a set of optimized strips.
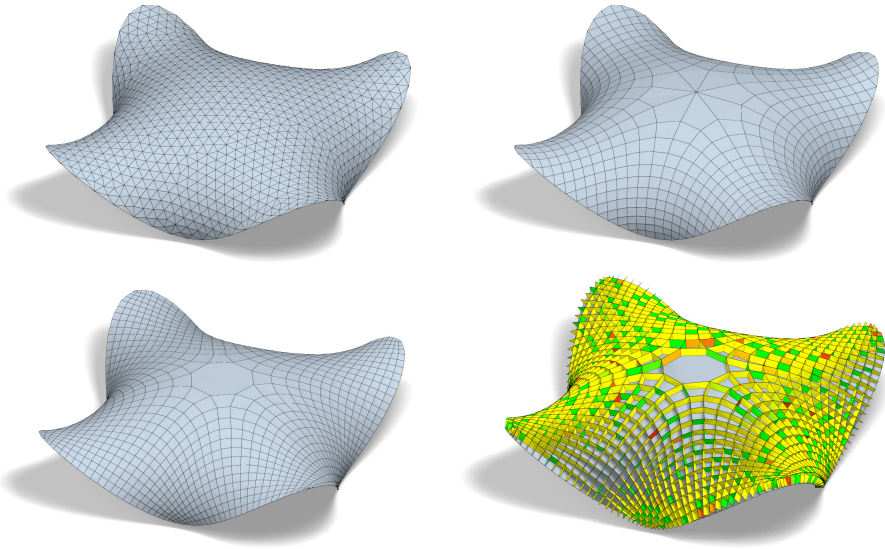
Figure 8: From left to right and top to bottom: Ocean reference surface, isothermic mesh, network of constant normal curvature curves, and the initial set of strips following the curve network.

We use the spherical vertex star property to explore the deformation behavior of the curve network. The network of diagonals extracted from the isothermic network M_1 (Figure 5) is a very good starting point to compute a discrete structure that satisfies this condition. Figure 7 shows the effect of reducing the radius of the red circle shown in the small inset while preserving edge lengths and the spherical vertex star condition with a fixed radius for all vertex spheres equal to the inverse of mean curvature H of the undoloid. The value of $H = 1.25$ was estimated on a triangle mesh representation of the unduloid reference surface.

Ocean. Reference surface ($H = 0.68$), isothermic mesh, curve network, and initial strips are shown in Figure 8. The set of optimized strips is shown in Figure 9. Strip quality deteriorates when approaching the boundary. This cannot be fixed by optimization of strips since rulings are determined by geodesic torsion τ_g and normal curvature κ_n of the guiding curves (which, in our case are uniquely defined by S and hence cannot be changed individually). As a remedy one needs to explore nearby reference shapes with a more favorable ratio of τ_g and κ_g along the curve network, or consider twisting lamellas during construction to allow deviation from a developable strip.

3   The Asymptotic Gridshell

The design and construction of the Asymptotic Gridshell simultaneously serve as motivation and case study for this paper. The structure illustrates the transfer from a purely geometrical concept to an architectural project, and presents the benefits
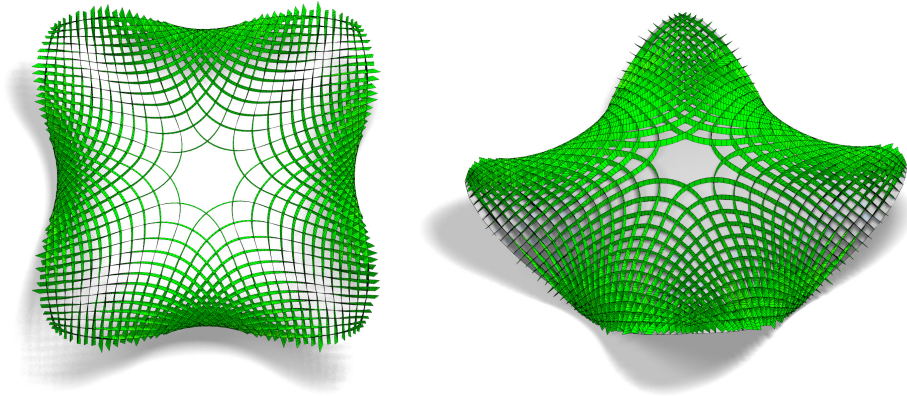
Figure 9: *Strips (of radius* 1.47*) after 2 rounds of subdivision, each followed by 20 iterations of guided projection.*

and challenges of designing with rigorous geometrical constraints, fabricating and assembling a strained lamella grid, and analysing its load-bearing behavior.

3.1   Design process

Surface.   The initial surface was designed using a fast digital routine for minimal surface approximation. While the algorithm implements the geometric requirements of a CMC surface, the designer is responsible for all other requirements like site, safety and functionality. A key challenge was to find a shape that would benefit an efficient shell-like load-transfer by approximating qualities of a funicular form. Manipulating the position and shape of two boundary curves, we created an intricate, mussel-shaped design with high double curvature and arch-shaped edges. Three curved horizontal supports nestle well along the complex site boundaries. The surface creates a circular oculus around an existing tree and opens two archways that allow circulation throughout the courtyard (Figure 10, left). Once the boundary curves were defined, the minimal surface was modeled more accurately as NURBS surface using the Rhino plugin TeDa (Philipp et al. (2016)).

Network and lamellas.   The network is designed along the paths of constant normal curvature (asymptotic curves) bisecting an isothermic principal curvature network (Section 2.2). This produces an almost square cell layout which is beneficial both structurally and graphically (Figure 10, right). Furthermore, the diagonal alignment with the principal curvature directions creates advantages for future facade solutions with single-curved or planar quadrilateral panels (Liu et al. (2006)).

The lamella geometry was simply defined by the normal vectors **n** (Figure 3, right). This creates a well-defined ruled surface strip with straight intersections deviating from a truly developable surface. As a consequence, the structural strips are twisted during assembly and experience elastic strain.

The geometry of network and lamellas is dependent on the curvature of the surface.
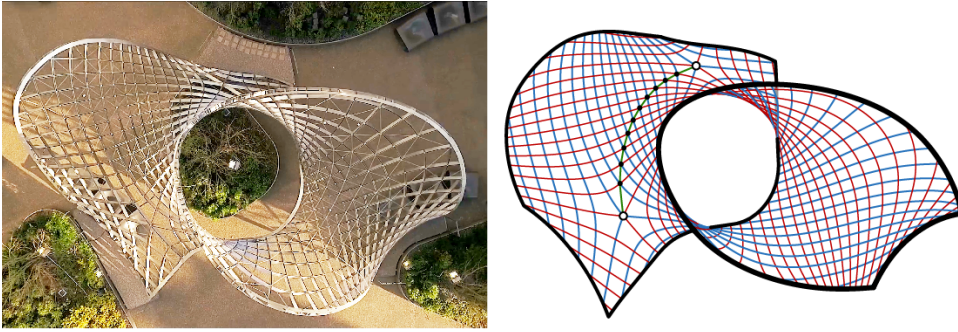
Figure 10: Left: The Asymptotic Gridshell was designed to fit an existing green courtyard. The arch-shaped design fosters the load-bearing behavior of a gridshell. Right: Two planar surface points create singularities which were iteratively adjusted during the design process to align in one principal curvature line. *(Image: Felix Noe)*

A high Gaussian curvature causes a high torsion of the lamellas which is limited by the elastic capabilities of the material. Planar surface points, on the other hand, create singularities within the network, and thus have a large impact on the layout and stability of the grid structure. Both factors were carefully adjusted by controlling the progression of boundary curves, re-computing the surface and testing the new network layout.

In the case of the Asymptotic Gridshell, there are two singularities on opposite sides, east and west of the central oculus. Both singularities are designed as congruent, regular, hexagonal nodes. They were arranged on the same principal curvature line. The grid density is determined by the subdivision of this connection axis.

3.2 Construction development

Implications of curvature. The three curvatures (normal curvature, geodesic curvature and geodesic torsion) within the structure are created either during fabrication (of circular lamellas) or during assembly (through elastic bending and twisting). The stresses due to elastic deformation are directly related to the curvature values. The $\mathbf{t}$, $\mathbf{u}$ and $\mathbf{n}$-vector resemble the x, y and z-axis of our lamellas profiles.

Let us first look at the gridshells of Frei Otto which mark the starting point of our construction development. Otto's design network is subject to all three curvatures. The timber lattice had to be constructed from slender, doubly symmetrical profiles in order to be bent and twisted around all axes. Any shape within the permissible bending radii can be built from such a grid.

Our curve networks, on the other hand, follow the paths of constant normal curvature. The grid can be constructed from straight or circular lamellas orientated perpendicular to the surface. As a consequence, no bending around the local y-axis (sideways vector) of the profiles is necessary during assembly. The geodesic curvature results in bending around the z-axis (normal vector), and the geodesic torsion creates twisting
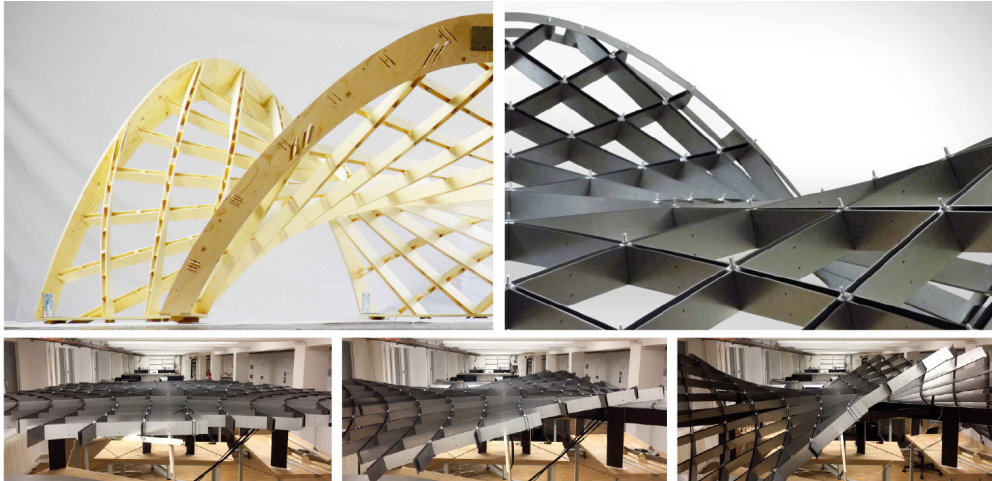
Figure 11: The structure was tested with two prototypes, one in timber and one in steel, each with an approx. 4×4 m span. Left: The lamellas of the timber prototype are arranged on separate levels to allow the use of uninterrupted profiles. Right: The lamellas of the steel prototype are interlocked in one level. They were first assembled flat and then transformed into the curved geometry.   *(Images: Eike Schling)*

of the lamellas around their x-axis (tangent vector). When choosing the profile thickness, the stiffness has to be adjusted to accommodate the maximum twist and minimal bending radii and keep deformation elastic.

In contrast to the timber gridshells of Frei Otto, the lamella grid is restricted to the family of shapes described in Section 2. This is due to the restricted deformation (i.e., high stiffness) in respect to the y-axis (i.e., constant normal curvature).

Post-stiffening strategy. If the elastic deformation of a material is used to construct a curved geometry, this inevitably poses the question of deflection and stability under self-weight and external loads. Increasing the bending stiffness is not an option if all elements are to be bent elastically into a curved geometry. Lienhard calls this discrepancy a "paradoxon that underlies all bending-active structures" (Lienhard (2014), p. 141).

These opposing requirements are solved by introducing two parallel layers of lamellas. Each layer is sufficiently slender to be bent and twisted elastically into its target geometry. Once the final geometry is installed, the two layers are coupled with shear blocks in regular intervals to increase the overall stiffness.

This construction technique was tested with two prototypes, one in timber and one in steel, each with an approx. 4×4 m span (Figure 11). The timber lamellas were bent individually and connected to a rigid edge-beam. The lamellas are arranged on two levels to allow for uninterrupted timber profiles. The steel prototype, on the other hand, was assembled flat (a benefit of straight lamellas) and subsequently transformed into the spatial geometry. Here the lamellas are slotted and interlocked at one level.

Figure 12: The typical grid joint is assembled with two parallel lamellas in each direction. Two standardized star-shaped washers fix the 90 degree intersection angle and create a central axis for the carriage bolt. The steel cables are also constructed in pairs and are fixed by a cross-shaped clamp. *(Images: Felix Noe)*

Grid joint. All nodes are congruent with an intersection angle of 90 degrees. They can thus be constructed with repetitive, orthogonal joints (Figure 12). At each intersection, two pairs of parallel lamellas are interlaced through perpendicular slots. The slots are twice as wide as the material thickness to allow a rotation of up to 60 degrees during assembly. The lamellas are locked by two star-shaped washers on top and bottom. A single carriage bolt and nut is used to fix each joint after they are transformed into the target geometry. An additional cross-shaped clamp fixes the diagonal cables. The Asymptotic Gridshell was constructed from 100 mm high and 1.5 mm thick, straight, stainless steel lamellas at parallel offset of 25 mm following the detailing and construction strategy of the steel prototype.

3.3 Construction process

Fabrication. Designing networks along constant normal curvature lines greatly simplifies fabrication: All lamellas are fabricated flat as either straight strips (on minimal surfaces) or circular strips (on any CMC-surface). The edge lengths from node to node, are the only variable information needed to produce fabrication drawings. The distances are simply marked along the standardized strips.

The lamellas of the Asymptotic Gridshell were laser-cut straight, which allowed for minimal offcuts and easy transport. The fabrication of washers and clamps was incorporated in the same laser-cutting procedure offering a cost-efficient production of all parts.

Erection process. The lamellas are slotted together to form a flat (for minimal surfaces) or spherical (for general CMC surfaces) girder (Figure 13). In this state, the lamellas display no geodesic torsion. The intersection angles are not yet constant. The joints are flexible and allow for a scissor movement. This lamella grillage can be deformed within a predefined family of shapes, one of which is the designed reference surface. It is found by enforcing a constant node angle of 90 degrees. The deformation behavior follows the same principles as described in Section 2.3 (Figure 7). This kinetic behavior is called a *compliant mechanism* (Howell (2002)). It enables an elastic erection process without formwork. Of course, this mechanism

Figure 13: The straight lamellas are interlocked by hand into flat segments. The segments are then transformed elastically into their designed shape by fixing each node to 90 degrees. Nine of these segments were prefabricated off site. (Images: Eike Schling)

Figure 14: Installation on site. The prefabricated segments of up to 400 kg, where positioned with a crane, temporarily supported, and bolted together by hand. To activate the structural behavior of a gridshell, the completed grid is braced diagonally and fixed at supports in vertical and horizontal direction. (Images: Andrea Schmidt)

is subject to gravity and other external loads and needs to be verified by selective measurements. Its further study is part of future research.

The Asymptotic Gridshell was prefabricated in nine individual segments (Figure 14). Each grillage was first assembled flat, then placed on a simple, cross-shaped stand and elastically deformed into its designated anticlastic curvature. Locking each node at 90 degrees and adding edge supports created rigid segments, which were then combined on site, like a large 3D puzzle. By fixing the supports and adding diagonal steel cables, this structure becomes an efficient, load-bearing gridshell.

3.4   The completed pavilion

The Asymptotic Gridshell is the first architectural structure that utilizes the geometric potentials of a constant normal curvature network on a constant mean curvature surface (Figure 16). The gridshell spans 9×12 m and covers an area of approx. 90 m^2. Its surface weight is approximately 18 kg/m^2, a total of 1.6 tons. A decisive factor for the aesthetical quality of both the shape and the lamella grid are owed to their formation process, following the curvature constraints of this design method. The slender lamellas create a gradient graphical effect with virtually full transparency at a straight view, and an almost opaque appearance at an inclined view (Figure 1).

3.5   Load-bearing behavior

FEM analysis.   The network geometry was modeled in Rhino/Grasshopper and exported as a discrete model to RFEM (Dlubal Software GmbH (2018)), where all necessary structural information was added. The geometric values of geodesic curvature and geodesic torsion were measured individually for each discrete element along the smooth curves and translated into strain loads in RFEM. This strategy enabled us to induce the residual stresses without modeling the actual assembly process (Figure 15). Due to intense twisting of the lamellas, additional normal stresses according to the effects of helix torsion are to be expected (Lumpe and Gensichen (2014) p. 118 – 128). These effects are not considered in the FE analysis which uses beam elements.

Global and local behavior.   We observed the hybrid load-bearing behavior of two competing mechanisms; a grillage and a gridshell. Due to the bending stiffness in their strong axis, the lamellas are able to act as a beam grillage. This is needed to account for the local planarity of the asymptotic curves (due to their vanishing normal curvature) and to stabilize the open edges. At the same time, the lamellas form a doubly-curved structure. Bracing this quadrilateral network with diagonal cables and creating fixed supports (in vertical and horizontal direction) activates behavior of a gridshell. Which of the two mechanism dominates is highly dependent on the design shape.

The arch-shaped boundaries of the Asymptotic Gridshell promote a shell-like behavior. Expanding the design spectrum to all CMC surfaces enables us to create synclastic shapes and further adapt to a funicular form.

Spannungen
Sigma-x [kN/cm^2]

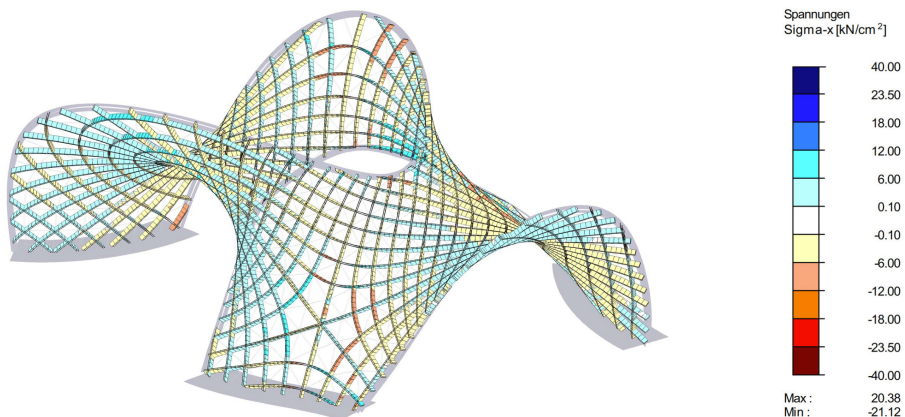|	
	40.00
	23.50
	18.00
	12.00
	6.00
	0.10
	-0.10
	-6.00
	-12.00
	-18.00
	-23.50
	-40.00

Max : 20.38
Min : -21.12

Figure 15: The load-bearing structure of the Asymptotic Gridshell. The lamellas are bent and twisted to form an anticlastic network with two singularities. The diagonal bracing is arranged at every second node. The horizontal supports adjust to the varying inclination angle of the edge beam. The diagram shows the surface stresses of the lamella grid resulting from both the elastic erection process and self-weight. All stresses stay within the elastic range.

Figure 16: The Asymptotic Gridshell was completed in October 2017. The structure is 5 m high and spans 9×12 m. It is built entirely from 1.5 mm-thick and 100 mm-wide steel lamellas.   *(Image: Felix Noe)*

The elastic erection process results in restraint (residual) stresses within the lamellas. Due to the low profile thickness, the initial bending moments stay low and have minor effects on the global behavior. However, compression of these curved elements increases the bending moment in their weak axis. The strategy of doubling and coupling lamellas is therefore essential to control local buckling.

The optimal orientations for compression and tension elements of a gridshell run along the principal stress trajectories. However, in our method, we choose to follow a geometrically optimized orientation along the directions of constant normal curvature, taking into account an increase of stresses.

4   Conclusion

Combining repetitive curvature parameters with an elastic construction holds great potentials for the fabrication, assembly and load-bearing behaviour of strained gridshells.

The technical requirements (straight or circular lamellas, congruent nodes) translate nicely into differential geometric characterizations of the curve networks and reference surfaces realizable with this approach. They even motivated the development of novel discrete structures (quad meshes with spherical vertex stars) which deserve interest from a purely geometric perspective.

The geometric properties greatly simplify the construction process: The lamellas have a beneficial orientation orthogonal to the design surface. They can be fabricated flat and straight or with a constant radius. All joints are identical and orthogonal. The elastic erection process takes advantage of a compliant mechanism, determining the design shape without formwork.

The elastic behavior, however, poses the challenge to avoid deflections and instability under self-weight and external loads. This paradoxon of bending-active structures was addressed within the design and construction process.

Even though our structures can only assume CMC surfaces, a substantial freedom in the design process remains with the potential to adjust to architectural and structural requirements.

Future Research.   Meshes with spherical vertex stars are a novel surface discretization which opens up new avenues of research in discrete differential geometry.

Our study also opens up two promising research fields that combine the disciplines of mathematics, architecture and engineering: (i) the investigation of the kinetic behaviour of elastic grids (compliant mechanisms) and the dependency of geometry and mechanics therein, (ii) the optimization of surfaces for both geometric requirements (like constant mean curvature) and structural performance (for shell structures).

Finally, we aim to develop further construction techniques and facade solutions for strained gridshells built from straight and circular lamellas.

References

Bobenko, A. I. and Y. B. Suris (2008). *Discrete Differential Geometry: Integrable Structure*. American Mathematical Society.

Burkhardt, B. (Ed.) (1978). *IL13: Multihalle Mannheim*. Stuttgart: Institut für leichte Flächentragwerke (IL)/Karl Krämer Verlag.

Dlubal Software GmbH (2018). RFEM 5. `www.dlubal.com`.

Evolute GmbH (2008–2018). EvoluteTools T.MAP. `www.evolute.at`.

Howell, L. L. (2002). *Compliant Mechanisms*. New York: Wiley & Sons.

Jimenez, M. R., C. Müller, and H. Pottmann (2018). Discretizations of surfaces with constant ratio of principal curvatures. *Discrete & Computational Geometry*. to appear.

Lienhard, J. (2014, April). Bending-active structures : form-finding strategies using elastic deformation in static and kinetic systems and the structural potentials therein.

Liu, Y., H. Pottmann, J. Wallner, Y.-L. Yang, and W. Wang (2006, July). Geometric modeling with conical meshes and developable surfaces. *ACM Trans. Graph. 25*(3), 681–689.

Lumpe, G. and V. Gensichen (2014). *Evaluierung der linearen und nichtlinearen Stabstatik in Theorie und Software: Prüfbeispiele, Fehlerursachen, genaue Theorie*. Ernst & Sohn.

Philipp, B., M. Breitenberger, I. D'Auria, R. Wüchner, and K.-U. Bletzinger (2016). Integrated design and analysis of structural membranes using the isogeometric B-rep analysis. *Computer Methods in Applied Mechanics and Engineering 303*, 312 − 340.

Schiftner, A., M. Höbinger, J. Wallner, and H. Pottmann (2009). Packing circles and spheres on surfaces. *ACM Trans. Graphics 28*(5), #139,1–8. Proc. SIGGRAPH Asia.

Schiftner, A., N. Leduc, P. Bompas, N. Baldassini, and M. Eigensatz (2012). Architectural geometry from research to practice: The eiffel tower pavilions. In *Advances in Architectural Geometry*.

Schling, E. and R. Barthel (2017). Experimental studies on the construction of doubly curved structures. *Detail structure* (01), 52–56.

Tang, C., M. Kilian, P. Bo, J. Wallner, and H. Pottmann (2016). Analysis and design of curved support structures. In S. Adriaenssens, F. Gramazio, M. Kohler, A. Menges, and M. Pauly (Eds.), *Advances in Architectural Geometry 2016*, pp. 8–23. VDF Hochschulverlag, ETH Zürich.

Tang, C., X. Sun, A. Gomes, J. Wallner, and H. Pottmann (2014). Form-finding with polyhedral meshes made simple. *ACM Trans. Graphics 33*(4). Proc. SIGGRAPPH.